TRANSITION METAL COMPLEXES OF 1,2,4-TRIAZOLE: ELECTRONIC AND MAGNETIC STUDIES

S. ZAYDOUN* and M. SAIDI IDRISSI

Laboratoire de Spectroscopie Infrarouge, Departement de Chimie, Faculté des Sciences, Université Mohammed V, Rabat, Morocco

A. ZRINEH

Laboratoire de Chimie Physique Générale, Département de Chimie, Faculté des Sciences, Université Mohammed V, Rabat, Morocco

and

B. AGRICOLE and C. GARRIGOU-LAGRANAGE

Centre de Recherche Paul Pascal, C.N.R.S., 33600, Pessac, France

Abstract—Manganese(II), iron(II), cobalt(II), nickel(II) and copper(II) halide complexes with 1,2,4-triazole as a ligand were synthesized and studied. Their structures were discussed on the basis of electronic and magnetic data. The electronic spectra of the compounds prepared (MX_2TA: M = Fe, Co, Ni, Cu, X = Cl; M = Co, Ni, Cu, X = Br; MX_2TA_2: M = Co, Ni, Cu, X = Cl; M = Mn, Co, Ni, X = Br; TA = 1,2,4-triazole) were analysed in the range 5000–50,000 cm^{-1}. The values obtained for D_q and B and the room temperature magnetic moments are consistent with a pseudo-octahedral arrangement for the metal. This implies that the complexes are polynuclear, probably polymeric. Using variable temperature magnetic susceptibility data, the parameters C, g and θ were determined. The iron, cobalt and copper compounds studied exhibit an antiferromagnetic interaction with a particular magnetic behaviour for CuX_2TA_2 compounds. NiX_2TA complexes show a ferromagnetic exchange coupling. Moreover, a sharp maximum is observed in the χ_p vs T plots of these two compounds at temperatures below that at which the ferromagnetic intra-chain interactions operate.

1,2,4-Triazole (TA) is of considerable interest as a ligand because of its presence in many fungicidal,[1] herbicidal[2] and pharamaceutical[3] compounds. Their activity is enhanced if TA exists as a salt or a metallic complex.[4–6] Some of our previous papers were concerned with structural studies in the solid state of salts of this compound and related derivatives,[7–10] whereas solutions of TA complexes were the subject of electrochemical and electronic paramagnetic resonance studies.[11] The object of the pre-

sent work is to study complexes of metallic halides with TA, having the overall composition μ-dihalogeno-μ-1,2,4-triazole metal(II) (MX_2TA) or dihalogeno-bis(μ-1,2,4-triazole)metal(II) (MX_2TA_2).

Some halide complexes of TA have been described previously. A polynuclear structure is proposed for $CuCl_2TA$,[12] as shown in Fig. 1. Copper ions are bridged with two chloride ions and 1,2-bicoordinating triazole ligand. $CuBr_2TA$ complex is isomorphous with $CuCl_2TA$.[13] The magnetic properties of these two compounds have been studied in detail[14–16] and their ligand-field spectra have been published.[17] Their experimental data, obtained
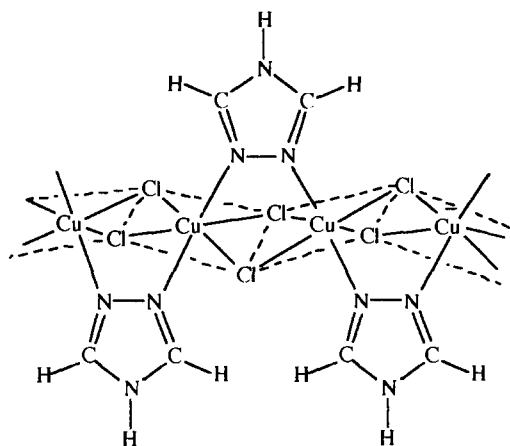
---

* Author to whom correspondence should be addressed.

Fig. 1. Simplified chain structure of CuCl$_2$TA in the solid state.[12]

by us, are given in this paper for a comparison with CuX$_2$TA$_2$ complexes. Except for the fragmentary study of CoCl$_2$TA$_2$, [NiCl$_2$TA$_2$]·1/2H$_2$O and CuCl$_2$TA$_2$ complexes done by Lavrenova *et al.*,[18] no paper on other halide complexes with TA of 1:1 or 1:2 stoichiometry exists in the literature. Our aim is to give a systematic investigation of the ligand-field spectra and the magnetic properties of MX$_2$TA and MX$_2$TA$_2$. A vibrational study of these complexes will be the subject of later papers.

EXPERIMENTAL

Starting materials

All chemicals and solvents were of pure quality and used without any further purification.

Synthesis of the complexes

The MX$_2$TA complexes were prepared by mixing acidic ethanolic solutions (2 M) of metal salts and ligand in stoichiometric quantities. The MX$_2$TA$_2$ complexes were obtained after adding metallic salts to excess of TA in an acidic ethanolic solution (0.2 M). The compounds were washed with ethanol and ether and dried in a desiccator.

Physico-chemical measurements

The stoichiometry of the compounds obtained was confirmed by carbon, hydrogen, nitrogen, halogen and metal analyses. X-ray powder diagrams were collected on a type CGR theta 60 diffractometer using Cu—$K_{\alpha 1}$. Thermogravimetrical analysis (TGA) curves were recorded with a Setaram thermobalance. Electronic spectra were studied in

the range 2000–200 nm with a Perkin–Elmer model 330 recording spectrophotometer using the diffuse reflectance accessory and magnesium oxide as reference. The reflectance spectra were obtained from pressed discs of pure compounds.

A classical Faraday balance with a temperature variable accessory was used to obtain magnetic measurements from room temperature to liquid helium temperature. The field strength used was between 1500 and 13,550 G. To obtain paramagnetic susceptibilities (χ_p), observed molar susceptibilities were corrected for diamagnetism of constituent atoms using Pascal's constants (χ_d, in 10^{-6} cgsu mol^{-1})[19] and for temperature-independent paramagnetism (χ_{tip}, in 10^{-6} cgsu mol^{-1}) calculated with the following relations:[20]

$$8N\mu_B{}^2/10D_q \quad \text{for} \quad A_2 \text{ ground terms}$$
$$4N\mu_B/10D_q \quad \text{for} \quad E \text{ ground terms}$$
$$0 \quad \text{for} \quad A_1 \text{ ground terms}$$

and ignored for T ground terms.

The D_q values were taken from ligand-field spectra. The effective magnetic moments were obtained using the relation:[21]

$$\mu_e = (8\chi_p T)^{1/2}.$$

RESULTS AND DISCUSSION

A list of the complexes prepared, their colours, elemental analyses, diffraction type and some lattice parameters is given in Table 1. It is seen from this table that the complexes of the same series are isomorphous. All the complexes are soluble in highly coordinating solvents such as dimethylformamide and dimethylsulphoxide and undergo complete solvolysis.[11] So, studies in solution are precluded.

The 1:2 nickel(II) complex was subjected to thermoanalytical experiments up to 600°C. The onset of weight loss on the TGA curves is at about 80°C. A loss of 5.23% agreed with the presence of one H$_2$O molecule in this compound.

Ligand-field spectra

Table 2 lists the assignments of charge transfer and π–π^* transitions. In Table 3 the ligand-field band energies and the assignments of d–d transitions are given. The calculated ligand-field parameters are given in Table 4.

All the compounds studied show relatively intense bands in the UV and the near-UV region. The highest energy band is attributed to the π–π^* triazole transition. Its energy decreases by complexation, as in pyrazine complexes.[22] It also decreases from chlorides to bromides (Table 2). The

Table 1. Complexes of TA, analyses, colours, X-ray types and lattice parameters calculated on the assumption of the monoclinic group space $I2/c$

Complex	Carbon[a]	Hydrogen[a]	Nitrogen[a]	Halogen[a]	Metal[a]	Colour	X-ray type[b]	Lattice parameters			
								a (Å)	b (Å)	c (Å)	β (°)
MnBr$_2$TA$_2$	14.0(13.6)	1.7(1.7)	23.9(23.8)	45.5(45.3)	15.5(15.6)	white	B				
FeCl$_2$TA	12.3(12.3)	1.9(1.5)	21.1(21.5)	35.4(36.2)	28.2(28.5)	yellow	A	6.92	11.61	7.25	96.96
CoCl$_2$TA	12.2(12.1)	1.6(1.5)	21.2(21.1)	35.2(35.7)	29.1(29.6)	violet	A	6.85	11.59	7.17	95.27
CoBr$_2$TA	8.3(8.4)	1.1(1.1)	14.3(14.6)	55.9(55.5)	19.2(20.5)	violet	A	6.97	12.59	7.93	65.73
CoCl$_2$TA$_2$	17.9(17.9)	2.3(2.3)	30.2(31.4)	26.4(26.5)	21.3(22.0)	pink	B				
CoBr$_2$TA$_2$	13.7(13.5)	2.1(1.7)	23.2(23.6)	42.7(44.8)	15.6(16.5)	pink	B				
NiCl$_2$TA	12.3(12.1)	1.9(1.5)	21.0(21.2)	35.2(35.7)	28.1(29.6)	green	A	6.86	11.47	7.14	96.40
NiBr$_2$TA	8.4(8.4)	1.3(1.1)	14.6(14.6)	55.8(55.6)	20.1(20.4)	green	A	6.88	12.31	7.13	96.80
[NiBr$_2$TA$_2$]·H$_2$O	13.0(12.8)	2.0(2.2)	22.5(22.4)	44.7(42.7)	15.7(15.7)	lilac	B				
CuCl$_2$TA	12.1(11.8)	1.4(1.5)	20.7(20.7)	34.8(34.8)	31.0(31.2)	green	A	6.82[c]	11.40	7.12	96.68
CuBr$_2$TA	8.3(8.2)	1.1(1.0)	14.5(14.4)	54.1(54.7)	21.5(21.7)	brown	A	6.94	12.58	7.99	65.23
CuCl$_2$TA$_2$	17.7(17.6)	2.3(2.2)	30.7(30.8)	26.1(26.0)	23.0(23.3)	light blue	B				
CuBr$_2$TA$_2$	13.2(13.3)	1.8(1.7)	23.1(23.2)	44.2(44.2)	17.8(17.6)	blue-green	B				

[a] Found (calculated).
[b] A or B are used to differentiate diffractogram types.
[c] Literature values are $a = 6.81$, $b = 11.39$, $c = 7.13$ Å and $\beta = 96°58'$.[12]

Table 2. Assignments of charge transfer and π–π* transitions (cm^{-1})

Complex	X → M	M → N	π–π*
MnBr$_2$TA$_2$	—	—	41,150
FeCl$_2$TA	—	29,600	(38,750)^a
CoCl$_2$TA	—	31,950	(35,950)
CoBr$_2$TA	—	28,350	(35,350)
CoCl$_2$TA$_2$	—	33,350	40,000
CoBr$_2$TA$_2$	—	30,050	39,550
NiCl$_2$TA	36,650	—	38,750
NiBr$_2$TA	31,950	—	37,300
[NiBr$_2$TA$_2$]·H$_2$O	34,700	—	40,000
CuCl$_2$TA	28,350	34,150	38,750
CuBr$_2$TA	22,300	29,150	38,750
CuCl$_2$TA$_2$	30,750	—	40,800
CuBr$_2$TA$_2$	25,750^b	—	—

^{a}Shoulder.

^{b}Very broad.

X → M and M → N electronic transfer transitions are assigned on the basis that the X → M frequency increases from manganese(II) to copper(II)[23] and from chloride to bromide,[24,25] while the M → N transfer increases from copper(II) to manganese(II).[23] Table 2 shows that when the number of halides decreases and that of nitrogens increases in the chromophores, the X → M and the M → N transfers decrease.

Manganese(II) *complex*. The shapes and positions of the bands correspond with octahedrally surrounded manganese(II) ions in the high spin state, having the $^6A_{1g}$ ground state.[21,26] Using the energy level diagrams and literature data,[27] all the other bands are assigned as in Table 3. The two bands observed at ca 6150 and 5800 cm^{-1} are due respectively to the overtones 2ν(CH) and 2ν(NH) of the TA ligand.[28,29]

The calculation of the ligand-field parameters D_q and B was performed by Lever's energy equations for the $^6A_{1g}$, $^4T_{1g}(G)$, $^4T_{2g}(G)$ and $^4A_{1g}(G)$ states.[26] The values of D_q, B[26] and D_q/B[30] are in agreement with the octahedral geometry proposed.

Iron(II) *complex*. The two broad bands observed for FeCl$_2$TA in the near-IR region are typical of pseudo-octahedral iron(II) compounds (Table 3).[21,26,31] They result from transitions introducing a ground electronic state derived from $^5T_{2g}$ to excited states derived from ^5E_g (in O_h symmetry).*

---

* The transitions for all the compounds are discussed, for convenience, in terms of O_h symmetry, although the actual symmetry can be lower.

According to literature data,[27] the highest energy component of the band assigned to the transition $^5T_{2g} \rightarrow {}^5E_g$ is a direct measure of the parameter D_q (Table 4).

Cobalt(II) *complexes*. The CoX$_2$TA and CoX$_2$TA$_2$ complexes have reflectance spectra typical of the cobalt(II) ion in a weak octahedral field. The two bands located at about 7000 and 10,000 cm^{-1} may be attributed to the components of the $^4T_{1g}(F) \rightarrow {}^4T_{2g}$ transition, which is split by a distortion from octahedral symmetry[32,33] (Table 3). The great intensity of the band attributed to the $^4T_{1g}(F) \rightarrow {}^4A_{2g}$ transition is explained by the existence of a tetragonal distortion.[21,34] The intense band assigned to the $^4T_{1g}(F) \rightarrow {}^4T_{1g}(P)$ transition is commonly split into a number of components interpreted essentially by a low symmetry effect and the occurrence of quartet–doublet transitions.[35] According to the energy level diagram of a d^7 ion in a weak octahedral field, the energy of the doublet states around $^4T_{1g}(P)$ increases with increasing D_q.

The D_q and B values, obtained using the method of calculation of Reedijk et al.[36] are in accordance with the octahedral geometry proposed (Table 4). The D_q values observed for CoX$_2$TA and CoX$_2$TA$_2$ are near those calculated for the CoX$_4$N$_2$ and CoX$_2$N$_4$ chromophores, respectively, using the rule of average environment established by Jorgensen[37] and the values of the CoCl$_6$, CoBr$_6$[26] and CoN$_6$[39] chromophores.

The spin-orbit coupling parameter λ is estimated for octahedral cobalt(II) complexes using the equation:[36]

$$\lambda = -0.168B^2/D_q.$$

As expected, its value is less than the free gaseous cobalt(II) ion and is explained, according to literature data,[33,37] by the covalent character of metal–ligand bonds.

Nickel(II) *complexes*. The general features of their reflectance spectra are consistent with a pseudo-octahedral structure and are similar to spectra published elsewhere.[39,40] As expected,[41,42] the ratio of the second and first transition energies is around 1.66. The shoulder on the lowest energy side of the second d–d band is probably due to the spin-forbidden transition $^3A_{2g} \rightarrow E_g(D)$.

The spectrum of [NiBr$_2$TA$_2$]·H$_2$O is complicated by many splittings of bands. It is similar to those reported for NiCl$_2$(thiazole)$_4$,[32] NiBr$_2$ (isoquinoline)$_4$[39] and NiCl$_2$(pyridine)$_4$,[40] in which organic ligands are in the equatorial plane and anionic ligands are in the apical positions. The structure of the $^3A_{2g} \rightarrow {}^3T_{1g}(F)$ band may be due, in addition to a distorted tetragonal crystal field, to the appearance of the spin-forbidden $^3A_{2g} \rightarrow {}^1E_g$

Table 3. Ligand-field band energies (cm^{-1}) and assignment of d–d transitions

Assignments

Complex			Band 1	Band 2	Band 3	Band 4	Band 5	Band 6
MnBr$_2$TA$_2$	2ν(CH) 6150	2ν(NH) 5800	$^6A_{1g}\to{}^4T_{1g}(G)$ 16,450	$^6A_{1g}\to{}^4T_{2g}(G)$ 21,150	$^6A_{1g}\to{}^4E_g(G),{}^4A_{1g}$ 23,350	$^6A_{1g}\to{}^4T_{2g}(D)$ 26,450	$^6A_{1g}\to{}^4E_g(D)$ 27,950	$^6A_{1g}\to{}^4T_{1g}(P)$ (31,450)^a
FeCl$_2$TA	2ν(CH) 6200	2ν(NH) 6200	$^5T_{2g}\to{}^5E_g$ 6200 10,350					
			$^4T_{1g}(F)\to{}^4T_{2g}$	$^4T_{1g}(F)\to{}^2T_{2g}$	$^4T_{1g}(F)\to{}^4A_{2g}$	$^4T_{1g}(F)\to{}^2T_{1g}(G)$	$^4T_{1g}(F)\to{}^4T_{1g}(P)$	
CoCl$_2$TA	2ν(CH) 6200	2ν(NH) 6200	6700 9800	(14,750)	16,450	(18,400)	19,300 (22,550)	
CoBr$_2$TA	6150	6150	6450 9450	(14,150)	15,650	(17,900)	18,950 (22,100)	
CoCl$_2$TA$_2$	6200	—	7100 10,250	(14,800)	(16,800)	(18,650)	20,150 (21,950)	
CoBr$_2$TA$_2$	6200	—	6700 9800	—	(16,600)	(18,600)	19,700 (22,100)	
			$^3A_{2g}\to{}^3T_{2g}$	$^3A_{2g}\to{}^1E_g(D)$	$^3A_{2g}\to{}^3T_{1g}(F)$	$^3A_{2g}\to{}^3T_{1g}(P)$		
NiCl$_2$TA	2ν(CH) 6250	2ν(NH) 6250	8800	(13,100)	14,550	24,200		
NiBr$_2$TA	6250	6200	8600	(13,000)	14,350	(23,950)		
[NiBr$_2$TA$_2$]·H$_2$O	6200	—	8300 12,000	(12,950)	14,000 17,300	(26,500)		
			$^2E_g\to{}^2T_{2g}$					
CuCl$_2$TA	2ν(CH) 6200	2ν(NH) 6200	(9950) 13,700					
CuBr$_2$TA	(6200)	(6200)	9550 13,550					
CuCl$_2$TA$_2$	6150	—	8750 14,800					
CuBr$_2$TA$_2$	—	—	8700 14,650					

^{a}Shoulders are given in parentheses.

Table 4. Ligand-field parameters

Complex	D_q (cm^{-1})	B (cm^{-1})	β^a	D_q/B	λ (cm^{-1})	$\lambda/\lambda_0{}^b$
MnBr$_2$TA$_2$	885	720	0.80	1.23		
FeCl$_2$TA	1035					
CoCl$_2$TA	870	795	0.82	1.09	-122	0.68
CoBr$_2$TA	850	795	0.82	1.07	-125	0.70
CoCl$_2$TA$_2$	1015	765	0.79	1.33	-97	0.54
CoBr$_2$TA$_2$	945	805	0.83	1.17	-115	0.70
NiCl$_2$TA	880	825	0.79	1.07	-209	0.64
NiBr$_2$TA	860	830	0.80	1.04	-216	0.67
[NiBr$_2$TA$_2$]·H$_2$O	975	860	0.83	1.13	-205	0.63
CuCl$_2$TA	1370					
CuBr$_2$TA	1355					
CuCl$_2$TA$_2$	1480					
CuBr$_2$TA$_2$	1465					

$^a\beta = B/B_0$; $B_0(Mn^{2+}) = 898$ cm^{-1}; $B_0(Co^{2+}) = 971$ cm^{-1}; $B_0(Ni^{2+}) = 1041$ cm^{-1}.
$^b\lambda_0(Co^{2+}) = -178$ cm^{-1}; $\lambda_0(Ni^{2+}) = 324$ cm^{-1}.

transition, which probably borrows intensity from the neighbouring triplet state.[41]

The band energies were used to calculate the D_q and B parameters by means of the energy equations of the triplet states given by Lever.[26] These parameters are in turn used for the calculation of λ:[43]

$$\lambda = -0.27B^2/D_q.$$

The obtained values of D_q and B, as well as the D_q/B ratio, are in good agreement with octahedral symmetry (Table 4). D_q and B values are similar to those of the corresponding cobalt(II) complexes, as expected from the adjacent positions of these two metals in the spectrochemical and the nephelauxetic series.[37] The D_q values calculated by the rule of average environment[37] and using the D_q values of the NiCl$_6$ and NiN$_6$ chromophores are consistent with the NiX$_4$N$_2$ and NiBr$_2$N$_4$ chromophores for the NiX$_2$TA and [NiBr$_2$TA$_2$]·H$_2$O complexes, respectively. The values of β and λ/λ_0 are indicative of significant covalent character in the metal–ligand bonds.

In addition to the ligand-field parameters, other parameters introduced by Moffitt and Ballhausen[44] can be calculated from literature equations for tetragonal octahedral nickel(II) complexes showing band splittings in their spectra.[40,45] The data obtained for the [NiBr$_2$TA$_2$]·H$_2$O complex,

$$D_t = 423 \text{ cm}^{-1}, D_s = 462 \text{ cm}^{-1},$$

$$D_q^{x,y} = 1200 \text{ cm}^{-1}, D_q^z = 460 \text{ cm}^{-1},$$

$$\delta[^3T_{1g}(P)] = 730 \text{ cm}^{-1},$$

show, as expected,[40] that the ligand-field strength of the equatorial groups is greater than for the axial

ones. The weak value of $\delta[^3T_{1g}(P)]$, which means the splitting of the $^3T_{1g}(P)$ state, is in accordance with the fact that the third d–d band is not split, despite the great tetragonal distortion.

Copper(II) *complexes.* The data obtained for CuX$_2$TA complexes are in accordance with Billing and Underhill's findings.[17]

The spectra of CuX$_2$TA$_2$ complexes exhibit two bands at about 8700 and 14,700 cm^{-1} typical of copper(II) ions in a tetragonally distorted octahedral environment (Table 3). They can be attributed to the components of the $^2E_g \rightarrow {}^2T_{2g}$ transition.[20] These results are different from those reported for CuCl$_2$TA$_2$ by Lavrenova *et al.*[18] and can be explained by the fact that the IR spectrum given by these authors shows a mixture of CuCl$_2$TA and CuCl$_2$TA$_2$.

The highest energy component of the $^2E_g \rightarrow T_{2g}$ band is taken as a measure for the ligand-field strength $10D_q$.[28,30]

Magnetic studies

The data obtained from magnetic studies are reported in Table 5. Figures 2 and 3 show the temperature dependence of the paramagnetic susceptibility χ_p, reciprocal paramagnetic susceptibility $\chi_p{}^{-1}$ and effective magnetic moment.

Manganese(II) *complex.* The magnetic moment at room temperature is near the spin-only value (Table 5) and is in agreement with the $^6A_{1g}$ ground state.

Iron(II) *complex.* The room temperature magnetic moment of FeCl$_2$TA is normal for high-spin octahedral iron(II).[46] It remains fairly constant

Table 5. Room temperature and variable temperature magnetic data

Complex	$\chi_d \cdot 10^6$ (mol^{-1})	$\chi_{pit} \cdot 10^6$ (mol^{-1})	$\chi_p \cdot 10^3$ (mol^{-1})	μ_e (μ_B)	μ_0 (μ_B)	θ (K)	C (emu kmol^{-1})	g
MnBr$_2$TA$_2$	−160.88	0	14.68	5.89	5.92			
FeCl$_2$TA	−102.44	ignored	12.20	5.37	4.90	−2.2	3.63	2.20
CoCl$_2$TA	−101.44	ignored	11.41	5.19	3.87	−13.1	3.73	2.82
CoBr$_2$TA	−121.44	—	10.01	4.86				
CoCl$_2$TA$_2$	−138.88	—	9.82	4.82				
CoBr$_2$TA$_2$	−158.88	—	8.59	4.50				
NiCl$_2$TA	−101.44	236.36	4.28	3.18	2.83	+19.8	1.19	2.18
NiBr$_2$TA	−121.44	241.86	4.06	3.10		+19.0	1.18	2.17
[NiBr$_2$TA$_2$]·H$_2$O	−171.88	213.33	3.59	2.91				
CuCl$_2$TA^a	−100.44	76.04	1.35	1.78	1.73	−10.1	0.42	2.12
CuBr$_2$TA^a	−120.44	76.75	1.24	1.71		−6.7	0.38	2.02
CuCl$_2$TA$_2$	−137.88	70.39	1.15	1.64		−172.4	0.47	2.24
CuBr$_2$TA$_2$	−157.88	71.00	0.82	1.39		−182.1	0.39	2.03

^{a}Literature data are: CuCl$_2$TA,[14] $\theta = -19.0$ K, $J = -12.3$ cm^{-1}, $C = 0.426$ emu kmol^{-1}, $g = 2.07$; CuBr$_2$TA,[15] $\theta = -6.7$ K, $J = -5.7$ cm^{-1}, $g = 2.10$.
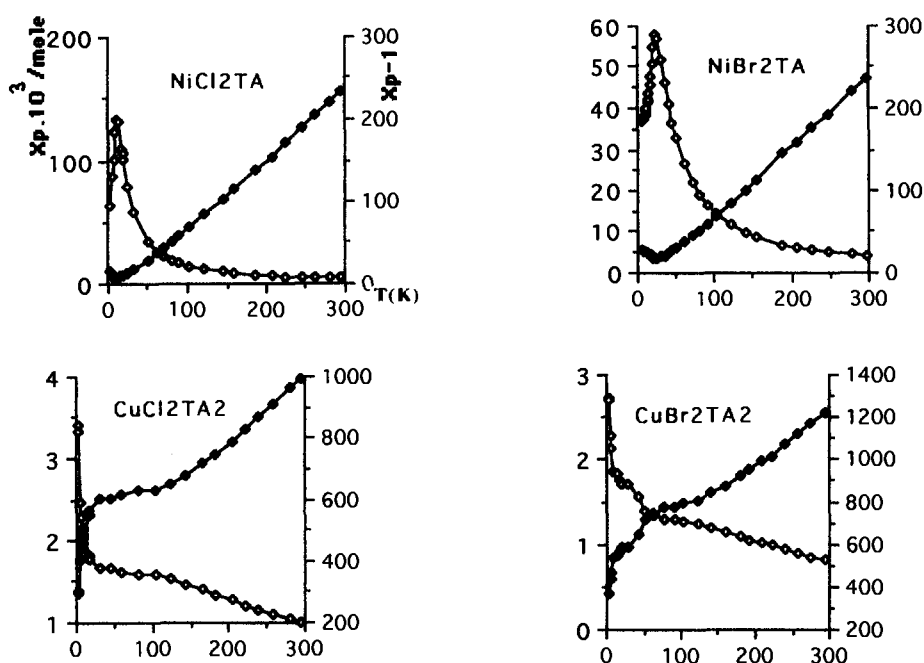

Fig. 2. Susceptibility and reciprocal susceptibility vs temperature of some triazole complexes.

down to approximately 50 K. This behaviour is consistent with a pseudo-octahedral high spin iron(II) compound in which the orbital degeneracy of the $^5T_{2g}$ state is lifted by a low symmetry crystal field.[27,28] The reciprocal susceptibility vs temperature plot implies Curie–Weiss behaviour. Because of the difficulty of recrystallizing the studied compounds, the magnetic effects observed below 25 K may only be apparent and due to impurities.

Cobalt(II) *complexes*. The magnetic moment of CoCl$_2$TA occurs in the range of octahedral cobalt(II).[46] The μ_e vs T and the θ sign (Fig. 3, Table 5) are consistent with the same suggestion as for FeCl$_2$TA. The room temperature moment values obtained for CoBr$_2$TA and CoX$_2$TA$_2$ are in accordance with pseudo-octahedral polynuclear complexes in which an antiferromagnetic coupling between the cobalt(II) ions exists.[32,33]

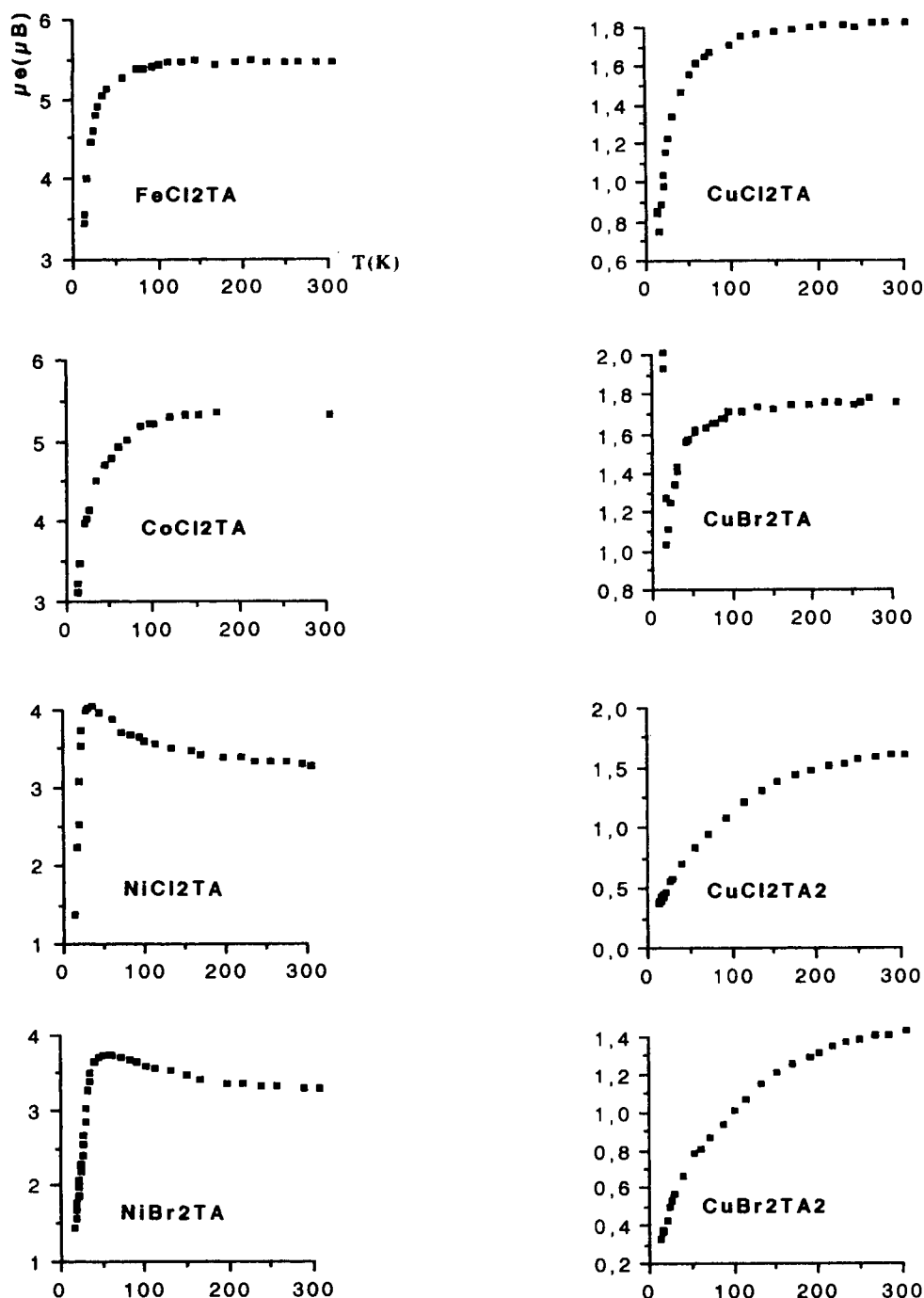*Nickel*(II) *complexes*. The room temperature

Fig. 3. Magnetic moment vs temperature of some triazole complexes.

magnetic moments of the nickel(II) complexes lie within the range 2.9–3.3 μ_B usually observed for octahedral nickel(II) compounds.[32,46] The values obtained below room temperature are above the spin-only moment and increase continually as the temperature decreases (Fig. 3). For NiX$_2$TA complexes, a maximum is observed at 18 and 45 K, respectively, for chloride and bromide, indicating a ferromagnetic exchange coupling between the met-

allic ions. This behaviour is comparable with that reported for other nickel(II) complexes[47] and is also implied by the positive θ values[48] (Table 5). A sharp maximum is observed in χ_p vs T plots at temperatures below that at which the ferromagnetic intra-chain interactions operate.

Copper(II) *complexes.* The room temperature magnetic moments of CuX$_2$TA compounds lie in the range 1.8–2.1 μ_B generally observed for cop-

per(II) complexes.[46] The χ_p and χ_p^{-1} vs T curves of the antiferromagnetic CuX_2TA complexes are compatible with those reported previously.[14-16]

In the CuX_2TA_2 complexes, a strong antiferromagnetic exchange coupling is present, as evidenced by the fact that the effective magnetic moment per copper ion is less than the spin-only value even at 295 K.[49] The decrease of μ_e when T decreases is more pronounced than for CuX_2TA and the θ values obtained between 295 and 150 K are indicative of a very strong antiferromagnetic coupling (Fig. 3, Table 5). The magnetic behaviour of χ_p and χ_p^{-1} is similar to that observed for the [Cu(NCS)(4-t-butyl-1,2,4-triazole)$_2$]NCS·1/2H$_2$O complex.[50] In accordance with this work, a polymeric structure is proposed for CuX_2TA_2 complexes. Two adjacent copper(II) ions are bridged by two 1,2-bicoordinating triazole ligands* in the equatorial plane and complete their hexacoordination by two halides in the axial positions. It has been shown previously[15] that the magnetic interaction in $CuCl_2TA$ takes place via the triazole heterocycles. So, the occurrence of more bridging triazoles in CuX_2TA_2 complexes enhances the magnitude of the superexchange interaction. In addition, the long metal–halogen bonds would allow an inter-chain magnetic interaction via hydrogen bonding between halides of a chain and "pyrrolic" hydrogens of triazole ligands of another chain, as was reported for the $CuCl_2(imidazole)_2$ complex.[51]

DISCUSSION

The small frequency shifts of d–d bands with changes of the anions X found for analogous complexes and D_q and B parameters can naturally be correlated with the position of the anions in the spectrochemical series and the sequence of the metallic ions in the spectrochemical and nephelauxetic series, respectively.[37] On the basis of the pseudo-octahedral geometry proposed, both halides and triazole ligands are bridged in MX_2TA series, probably giving a monodimensional chain structure like that of $CuCl_2TA$[12] (Fig. 1). For MX_2TA_2 complexes, the D_q values are consistent with a structure in which metallic ions are bridged by more triazole ligands than for MX_2TA complexes. The triazole ligands are in the plane of the octahedra and the anions are axial and terminal, as shown in

Fig. 4. A structure with coplanar triazole ligands would lead to a considerable steric hindrance between adjacent triazoles and some tilting is likely.

The great tetragonal distortion observed for nickel(II) and copper(II) compounds would result in longer M—X bonds which would be "semi-coordinated".[52] Then the M—N bonds shorten on going from chlorine to bromine (Pauling principle[52]) and the global ligand-field remains practically constant, as is seen from D_q values of analogous compounds with different halogens (Table 3).

Except for the nickel(II) complexes, all the compounds studied show an intra-chain antiferromagnetic behaviour. Recent papers reported that the most important structural feature which determines the type of superexchange is the MXM angle, where X is the bridging atom.[47,53] This angle, equal to 83.2° in $CuCl_2TA$,[12] is probably different in NiX_2TA complexes, leading to a different type of magnetic interaction.

As has been reported in the case of M(anion)$_2$ (pyrazine)$_2$ compounds[31] having a similar structure to that proposed for MX_2TA_2 complexes, because of the steric hindrance, the triazole rings should be tilted out of the equatorial plane. This gives rise to an important overlap and to a facile magnetic mechanism, in addition to the hydrogen bond magnetic pathway. However, in the absence of X-ray data, these suggestions must be considered speculative.

CONCLUSION

The geometry of the metallic ion in MX_2TA and MX_2TA_2 complexes is pseudo-octahedral. The complexes are polymeric and metallic ions are
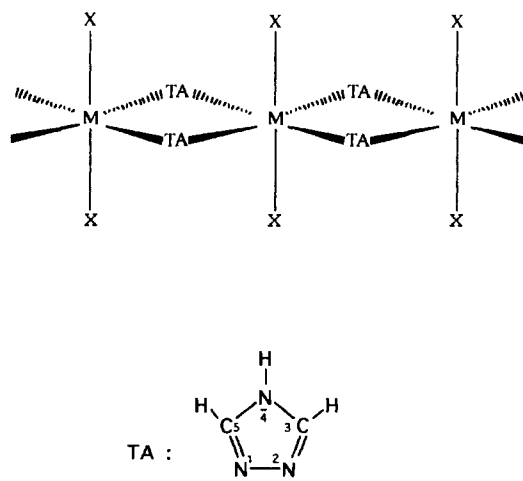

TA :

Fig. 4. Simplified chain structure proposed for MX_2TA_2 in the solid state.

---

*The 1,2-bicoordination was concluded from IR spectra.[29]

bridged by triazoles and halogens for MX_2TA and by more triazoles in the equatorial plane for complexes of the second series. The occurrence of magnetic interaction is confirmation of the bridged structures. The compounds studied generally exhibit antiferromagnetic coupling. The nickel(II) complexes show a ferromagnetic exchange interaction. The effect of minor modifications in the geometry around the nickel ion may be the origin of the different magnetic behaviours observed.

REFERENCES

1. P. H. Freeman, P. A. Worthington and W. G. Rathmell, Eur. Pat. Appl. EP 0044, 407 (1982).
2. J. L. Hilton, *J. Agric. Food Chem.* 1969, **17**, 182.
3. C. K. Joshi and K. Dubey, *Phamazie* 1979, **34**, 801.
4. H. O. Bayer, R. S. Cook and W. C. Von Meyer, U.S. Patent 3, 821, 376, June 28 (1974).
5. K. P. Parry, P. A. Worthington and W. G. Rathmell, Eur. Pat. Appl. 15, 756 (1980).
6. J. Singh and N. K. Singh, *Proc. Indian Acad. Sci. (Chem. Sci.)* 1984, **93**, 125.
7. M. Saidi Idrissi, H. Sauvaitre and C. Garrigou-Lagrange, *J. Chem. Phys.* 1983, **80**, 739.
8. S. Zaydoun, M. Saidi Idrissi and C. Garrigou-Lagrange, *Can. J. Chem.* 1987, **65**, 2509.
9. S. Zaydoun, M. Saidi Idrissi and C. Garrigou-Lagrange, *Spectrochim. Acta* 1988, **44A**, 1421.
10. S. Zaydoun, M. Saidi Idrissi, C. Garrigou-Lagrange and M. Gelize-Duvigneau, *J. Chim. Phys.* 1988, **85**, 957.
11. K. M. Kadish, Y. Deng, S. Zaydoun and M. Saidi Idrissi, *J. Chem. Soc., Dalton Trans.* 1990, 2809.
12. J. A. J. Jarvis, *Acta Cryst.* 1962, **15**, 964.
13. T. Asaji, H. Sakai and D. Nakamura, *Inorg. Chem.* 1983, **22**, 202.
14. M. Inoue, S. Emori and M. Kubo, *Inorg. Chem.* 1968, **7**, 1427.
15. S. Emori, M. Inoue and M. Kubo, *Bull. Chem. Soc. Japan* 1972, **45**, 2259.
16. Y. Lepine, V. Larochelle, A. Caille and J. L. Thompson, *Phys. Status Solidi (b)* 1979, **91**, K111.
17. D. E. Billing and A. E. Underhill, *J. Inorg. Nucl. Chem.* 1968, **30**, 2147.
18. L. G. Lavrenova, S. V. Larionov, Z. A. Grankina and V. N. Ikorskii, *Zh. Neorg. Khim.* 1983, **28**, 442.
19. G. Foex, *Constantes Selectionnées Diamagnétiques et Paramagnétiques.* Masson, Paris (1957).
20. C. J. Ballhausen, *Introduction of Ligand Field Theory.* McGraw-Hill, New York (1962).
21. F. A. Cotton and G. Wilkinson, *Advanced Inorganic Chemistry.* Interscience, London (1966).
22. H. W. Richardson and W. E. Hatfield, *J. Am. Chem. Soc.* 1976, **98**, 835.
23. A. B. P. Lever, *J. Chem. Educ.* 1974, **51**, 612.
24. D. E. Billing, A. E. Underhill, D. M. Adams and D. M. Morris, *J. Chem. Soc. (A)* 1966, 902.
25. J. C. T. Rendell and L. K. Thompson, *Can. J. Chem.* 1979, **57**, 1.
26. A. B. P. Lever, *Inorganic Electronic Spectroscopy.* Elsevier, Amsterdam (1968).
27. J. Reedijk, *Recl. Trav. Chim. Pays-Bas* 1969, **88**, 1451.
28. J. G. Vos, Thesis, Leiden (1978).
29. S. Zaydoun, Thesis, Rabat (1992).
30. A. B. P. Lever, *J. Chem. Educ.* 1968, **45**, 711.
31. G. Kolks, S. J. Lippard, J. V. Waszcazock and H. R. J. Lilienthal, *J. Am. Chem. Soc.* 1982, **104**, 717.
32. W. J. Eilbeck, F. Holmes and A. E. Underhill, *J. Chem. Soc. (A)* 1967, 757.
33. R. Battistuzi, *Polyhedron* 1985, **4**, 933.
34. P. D. Singh, N. K. Jha and L. K. Mishra, *J. Inorg. Nucl. Chem.* 1980, **42**, 282.
35. A. B. P. Lever and D. Ogden, *J. Chem. Soc. (A)* 1967, 2041.
36. J. Reedijk, W. L. Driessen and W. L. Groeneveld, *Recl. Trav. Chim. Pays-Bas* 1969, **88**, 1095.
37. C. K. Jorgensen, *Absorption Spectra and Chemical Bonding in Complexes.* Pergamon Press, Oxford (1964).
38. J. G. Haasnoot, G. Vos and W. L. Groeneveld, *Z. Naturfor.* 1977, **32b**, 1421.
39. D. M. L. Goodgame, M. Goodgame, M. A. Hitchman and M. J. Weeks, *J. Chem. Soc. (A)* 1966, 1769.
40. A. B. P. Lever, *Coord. Chem. Rev.* 1968, **3**, 119.
41. A. B. P. Lever, J. Lewis and R. S. Nyholm, *J. Chem. Soc.* 1964, 4761.
42. N. A. Daugherty and J. H. Swisher, *Inorg. Chem.* 1968, **7**, 1651.
43. J. Reedijk, P. W. N. M. Van Leeuwen and W. L. Groeneveld, *Recl. Trav. Chim. Pays-Bas* 1968, **87**, 129.
44. W. Moffitt and C. J. Ballhausen, *J. Inorg. Nucl. Chem.* 1956, **3**, 178.
45. G. R. Brubaker and D. H. Busch, *Inorg. Chem.* 1966, **5**, 2114.
46. A. Earnshow, *Introduction to Magnetochemistry.* Academic Press, London (1968).
47. J. S. Haynes, S. J. Rettig, J. R. Sams, R. C. Thompson and J. Trotter, *Can. J. Chem.* 1987, **65**, 420.
48. E. J. Duff and M. N. Hughes, *J. Chem. Soc. (A)* 1966, 477.
49. L. K. Thompson, T. C. Woon, D. B. Murphy, E. J. Gabe, F. L. Lee and Y. Le Page, *Inorg. Chem.* 1985, **24**, 4719.
50. L. R. Groeneveld, R. A. Le Fèbre, R. A. G. De Graaff, J. G. Haasnoot, G. Vos and J. Reedijk, *Inorg. Chim. Acta* 1985, **102**, 69.
51. J. A. C. Van Ooijen and J. Reedijk, *J. Chem. Soc., Dalton Trans.* 1978, 1170.
52. J. Hathaway and D. E. Billing, *Coord. Chem. Rev.* 1970, **5**, 143.
53. D. Ajo, A. Bencini and F. Mani, *Inorg. Chem.* 1988, **27**, 2437.